Article ID: 1000-324X(2018)07-0805-06 **DOI:** 10.15541/jim20170610

Enhanced Visible-light-driven Photocatalytic Activity of Multiferroic $KBiFe_2O_5$ by Adjusting pH Value

LI Jian[1], ZHANG Gang-Hua[2], FAN Li-Kun[2], HUANG Guo-Quan[1], GAO Zhi-Peng[3], ZENG Tao[1,2]

(1. College of Environmental and Chemical Engineering, Shanghai University of Electric Power, Shanghai 200090, China; 2. Shanghai Key Laboratory of Engineering Materials Application and Evaluation, Shanghai Research Institute of Materials, Shanghai 200437, China; 3. National Key Laboratory of Shock Wave and Detonation Physics, Institute of Fluid Physics, China Academy of Engineering Physics, Mianyang 621900, China)

Abstract: Multiferroic $KBiFe_2O_5$ was successfully prepared by a facile hydrothermal method. Its phase purity and morphology were investigated by powder X-ray diffraction (XRD) and field emission scanning electron microscopy (FE-SEM). The visible-light absorption was confirmed by UV-Vis diffuse reaction spectroscopy (UV-Vis DRS). Effect of pH value on visible-light-driven photocatalytic properties of $KBiFe_2O_5$ was evaluated by degrading rhodamine B (RhB) and methyl orange (MO). It can be found that lower pH value contributed to smaller average particle size. The D_{50} of the sample at pH 7 is about 10 times larger than that at pH 2. Acid condition is beneficial to the dispersion of $KBiFe_2O_5$ nanoparticles, which leads to an enhanced photocatalytic performance. Photocatalytic activity of $KBiFe_2O_5$ is significantly improved by decreasing pH value of the solution, which is attributed to the promoted dispersion of catalyst particles in the suspension and the enhanced adsorption of dye molecules on the catalyst surface.

Key words: $KBiFe_2O_5$; photocatalyst; visible-light irradiation; pH value

Traditional metal oxides or metal sulfides semiconductors, such as TiO_2[1-3], ZnO[4-5] and ZnS[6-7], have received considerable attentions due to their potential application for the degradation of organic contaminants and hydrogen generation from water[8-9]. However, due to the finite absorbance of the UV-light (~5% of the sunlight) and the fast recombination of the photogenerated carries[10], the large band gap E_g (>3 eV) and low conversion efficiency limit their practical application. Actually, the spontaneous polarization of ferroelectric materials can act as a homogeneous inner electric field which is beneficial to separating the photogenerated carriers[11-12]. Nevertheless, the E_g of most reported ferroelectric photocatalysts, such as $BiFeO_3$ (2.6 eV)[13] and Bi_2WO_6 (2.72 eV)[14], are still insufficient to absorb the entire solar spectrum. Therefore, many efforts have been devoted to promoting the photocatalytic performances of ferroelectric materials recently[15-18]. The optimal band-gap range for excellent light-absorbing materials is about 1.0 eV - 1.8 eV based on the energy distribution of the solar spectrum[19]. Most recently, several ferroelectrics have been reported with narrow E_g around 1.5 eV, such as $KBiFe_2O_5$[20] and $[KNbO_3]_{1-x}[BaNi_{1/2}Nb_{1/2}\text{-}O_{3-\delta}]_x$[21]. Contrast to the enhanced light absorption and promoted photoelectric response, few studies have given deep insight into their photocatalytic performance so far.

Commonly, the photocatalytic performances of the most photocatalysts have been demonstrated to be highly pH-dependent[22]. Under acidic condition, the enhanced photocatalytic activities have been achieved in several ferroelectric materials, such as $BiFeO_3$[23] and Bi_2WO_6[24]. It has been proposed that the concentration of H^+ on the catalyst surface at different pH values would affect the dispersion of catalyst particles and the absorption of dye molecules on catalyst surface, and thus influence the photocatalytic activity[23-25]. But there is no report on the effect of pH value on the photocatalytic properties of such ferroelectrics with narrow E_g. Although the primary photocatalytic activity of multiferroic $KBiFe_2O_5$ has been reported, the photocatalytic efficiency is still less than satisfactory. Therefore, enhanced photocatalytic performances can also be expected in these narrow-band-gap ferroelectrics by adjusting the pH value.

In this work, $KBiFe_2O_5$ has been employed as a candidate to investigate the role of pH value on the photocatalytic properties of the ferroelectric materials with

Received date: 2017-12-28; **Modified date:** 2018-03-30
Foundation item: National Natural Science Foundation China (51772184, 11704353); LSD Engineering Project (2016Z-04); Dean Fund of CAEP (YZJJLX2016001); CSS Project (YK2015-0602006); Shanghai Materials Genome Institute No.5 (16DZ2260605)
Biography: LI Jian(1990–), male, candidate of Master degree. E-mail: 18521099679@163.com
Corresponding author: ZENG Tao, professor. E-mail: zengtao@srim.com.cn; GAO Zhi-Peng, associate professor. E-mail: z.p.gao@foxmail.com

narrow E_g. Because of the mild reaction conditions and simple apparatus, hydrothermal synthesis has been utilized to synthesize the pure phase $KBiFe_2O_5$. The visible-light-driven photocatalytic properties under different pH values have been investigated by degrading the rhodamine B(RhB) and methyl orange (MO) dyes. The photocatalytic efficiency of $KBiFe_2O_5$ can be significantly improved by increasing the initial acidity of dye solution.

1 Experimental

As a typical preparation method of $KBiFe_2O_5$, 7.5 mL $Bi(NO_3)_3{\cdot}5H_2O$ (0.2 mol/L) and 15mL $Fe(NO_3)_3{\cdot}9H_2O$ (0.2 mol/L) were initially mixed in a beaker, then 50 g KOH was directly added into the mixture with constantly magnetic stirring. When the reaction mixture was cooled to room temperature in the air, it was then transferred into a 50 mL Teflon-lined stainless steel autoclave with 70% filling and heat-treated at 220℃ for 48 h. After the autoclave was cooled and depressurized, the product was collected and washed with deionized water and dried at 80℃ in air.

The purity and crystallinity of $KBiFe_2O_5$ were characterized by X-ray diffractometer (XRD) on Bruker D8 advance diffractometer operating with Cu Kα radiation. The crystal and morphology were checked by field emission scanning electron microscopy (FE-SEM). The optical absorption was measured using a UV-3100 Shimadzu ultraviolet-visible-infrared spectrophotometer. Photocatalytic performance was evaluated by degrading RhB and MO at various pH under visible-light-irradiation using a 500 W Xe lamp with a cut off filter for $\lambda \geqslant 420$ nm. The reaction temperature was kept at room temperature by cooling water to prevent any thermal catalytic effect. The distance between the liquid surface and the light source was about 10 cm. The initial pH of dye solution was adjusted by adding HCl and NaOH. For each run, 0.05 g of photocatalyst was added into 100 mL dye solution (10^{-5} mol/L). Prior to irradiation, the suspension was stirred in dark for 30 minutes to ensure adsorption/desorption equilibrium. After given irradiation times, 5 mL reaction solution was collected and centrifuged to remove the photocatalyst. Absorbance of the filtrates was measured by a Hewlett-Packard 8453 UV-Vis spectrophotometer (USA).

The photocatalytic capability of $KBiFe_2O_5$ powders was evaluated by degradation rate (D) of dye solution and the reaction kinetics of dye degradation, which was quantitatively described on the basis of a pseudo-first-order reaction model. These parameters can be calculated from the following equations[26]:

$$D(\%) = \frac{C_0 - C_t}{C_0} \times 100\% = \frac{A_0 - A_t}{A_0} \times 100\% \quad (1)$$

$$\ln \frac{C_t}{C_0} = kt \quad (2)$$

Where D(%) was the degradation rate of dye solution at time t, C_0 and C_t were the concentrations of dye solution at time t_0 and t respectively, A_0 and A_t were the absorbance of dye solution at time t_0 and t respectively. According to the Eq. (2), a plot of $-\ln(C_t/C_0)$ *versus* t will yield a slop of apparent rate constant (k, min^{-1}).

2 Results and discussion

The XRD patterns of as-grown $KBiFe_2O_5$ powders (Fig. 1) can be indexed to the orthorhombic space group $P2_1cn$ with cell parameters a = 0.7988(2) nm, b = 1.1819(2) nm, c = 0.5734(1) nm, which is identical to the simulated one using single-crystal data[20]. The excellent crystallinity of the sample has been confirmed by FE-SEM images as shown in Fig. 2(a). FE-SEM photograph shows clearly the material to be made up of rod-like single crystals, around 25 μm in width and 100 μm–200 μm in length. For photocatalytic experiments, the crystalline $KBiFe_2O_5$ was first grinded into nano particles around 100 nm–200 nm (as shown in Fig. 2(b)) through high speed ball milling, so as to improve its specific surface area for photocatalytic activity. The diffuse reflectance spectra of $KBiFe_2O_5$ and the extrapolated band gap are shown in Fig. 2(c) and (d). Based on the Kubelka-Munk (K-M) function[27], the band-gap of as-prepared $KBiFe_2O_5$ can be determined as 1.63 eV, which is consistent with the data reported previously[20].

To reveal the effect of pH value on the photocatalytic performance of $KBiFe_2O_5$, the photocatalytic decompositions of RhB and MO have been carried out at different

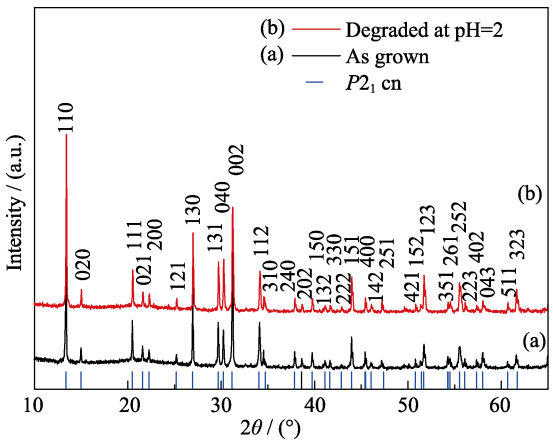

Fig. 1 XRD patterns of as-grown $KBiFe_2O_5$ and after degradation at pH 2

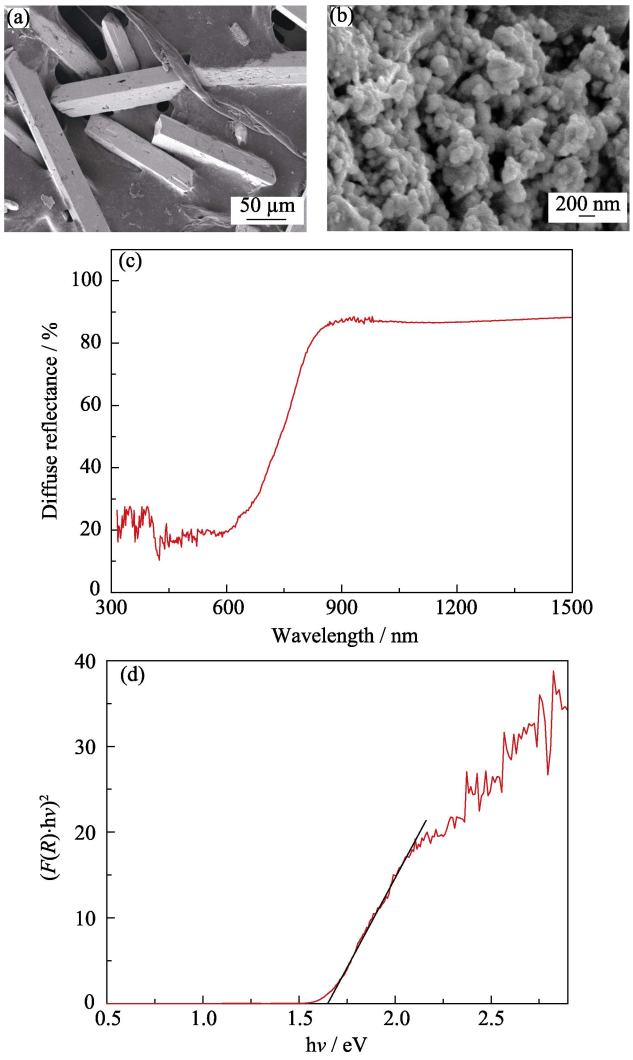

Fig. 2　FE-SEM image (a, b), diffuse reflection spectrum (c), and $(F(R)h\nu)^2$ against $h\nu$ (d) of $KBiFe_2O_5$

pH values under visible-light illumination. As shown in Fig. 3(a) and (b), the blank experiments were carried out at pH=7 (blank 1) and pH=2 (blank 2) respectively, which demonstrated the stabilities of RhB and MO under visible-light irradiation without photocatalyst. The degradation rates of RhB and MO dyes with $KBiFe_2O_5$ were relatively low at neutral or alkaline condition. By decreasing the pH value, the photocatalytic efficiency of $KBiFe_2O_5$ can be improved extremely. At pH = 2, the RhB dye can be degraded completely within only 20 min, whereas the degradation rate can reach only 30% at pH = 7 after 2 hours of visible-light irradiation. The degradation efficiency of MO dye increases notably from the original ~ 21% at pH = 7 to 99.5 % at pH = 2 after 2 h of visible-light irradiation. Fig. 3(c) and (d) show the corresponding temporal evolutions of all the absorption spectra of the RhB and MO solution degraded by $KBiFe_2O_5$ under Xe lamp light irradiation at pH = 2.

Moreover, the corresponding rate constants k have also been calculated by using pseudo first-order reaction kinetics[28] as shown in Fig. 4(a) and (b). With decreasing pH value, the rate constant k increased obviously, corresponding to the trend of the degradation efficiency. Furthermore, the photostability of $KBiFe_2O_5$ was confirmed by the photodegradation circulating tests of RhB and MO dyes at pH = 2 (Fig. 4(c) and (d)). After five cycling tests for the photodegradations of RhB and MO dyes, the high photocatalytic activity reveals that $KBiFe_2O_5$ possesses an excellent photostability, which also confirmed by the XRD pattern of reused $KBiFe_2O_5$ withoat additional Bragg peak.

The photodegradation results demonstrated that the pH value of dye solution has a significant influence on the photocatalytic performance of $KBiFe_2O_5$. The photocatalytic degradation efficiency (k = 0.15196) for RhB at pH = 2 obtained in present work is better than the one reported in other ferroelectric photocatalysts, such as $BiFeO_3$[23] (k = 0.0692 at pH = 0.5) and Bi_2WO_6[24] (k = 0.02035 at pH = 3.2). The enhanced photocatalytic activity by increasing the acidity of dye solution has also been demonstrated by degrading RhB with $BiFeO_3$[23] and MO with $Bi_4Ti_3O_{12}$[25]. The mechanism of pH value's influence on the dye degradation can be explained as follows: the pH value of the solution can affect the dispersion of catalyst particles in suspension and the adsorption of dye molecules on catalyst surface, which have important influence on their photodegradation activity. The better dispersion of catalyst particles in the suspension will create more active sites to improve the degradation efficiency of catalyst. The adsorption of dye molecules on the catalyst surface will promote the reaction rate due to the direct charge transfer. It has been demonstrated that the RhB is an anion dye while MO is a cationic dye[23,25]. So, in the RhB-$KBiFe_2O_5$ suspension, a large amount of positive charges accumulated on the surface of $KBiFe_2O_5$ at acid condition, which was beneficial to the dispersion of the catalyst powders, led to a significant enhance of photodegradation efficiency. In the MO-$KBiFe_2O_5$ suspension, the acid condition would be conductive to the absorption of the negative MO molecules on the surface of $KBiFe_2O_5$, and thus improved the photodegradation efficiency of $KBiFe_2O_5$.

The effect of pH on the dispersion of $KBiFe_2O_5$ particles in the suspension was verified through granularity analysis using laser particle size analyzer. The average particle sizes (D_{50}) of $KBiFe_2O_5$ at different pH value were listed in Table 1. It can be found that lower pH value contributed to smaller average particle size. The D_{50} of the sample at pH=7 is about 10 times larger than that at pH=2, which is attributed to the agglomeration of the nanoparticles caused by the effect of Vander Waals force in the suspension with higher pH value. Thus, the acid

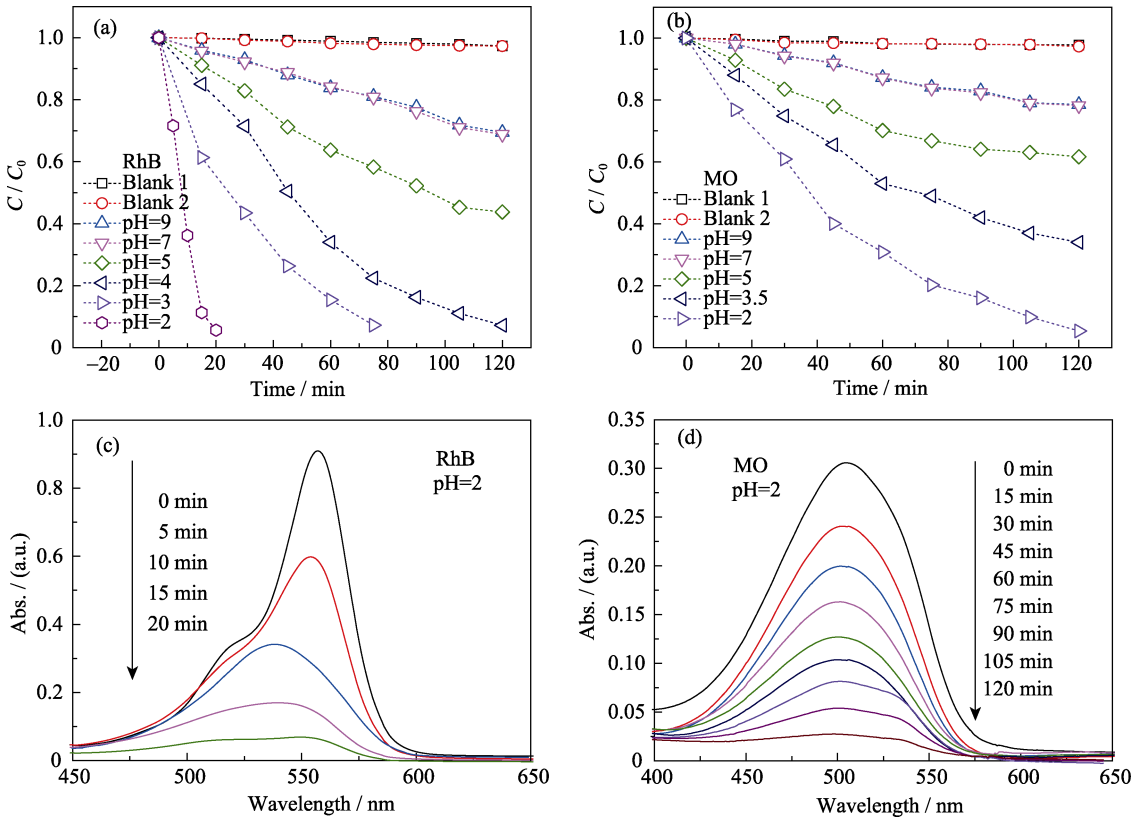

Fig. 3 Degradation rates of RhB (a) and MO (b) using $KBiFe_2O_5$ at different pH values, and absorption changes of RhB (c) and MO (d) solution in photocatalytic process at pH 2

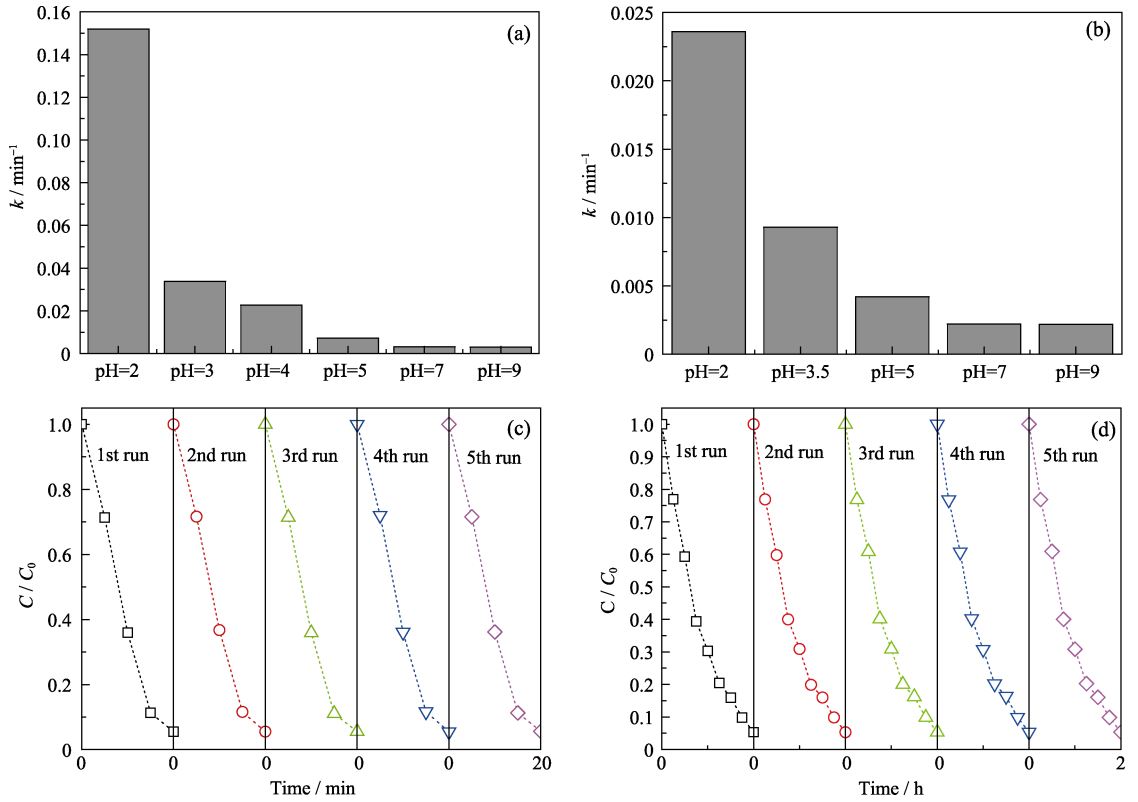

Fig. 4 Corresponding reaction rate constant k for the photocatalytic degradation of RhB (a) and MO (b) by $KBiFe_2O_5$ at various pH value, and circulating runs in the photocatalytic degradation of RhB (c) and MO (d) at pH 2

Table 1　Average particle size of $KBiFe_2O_5$ in suspensions at various pH values

Sample	pH=2	pH=3.5	pH=5	pH=7
D_{50}/μm	0.341	0.654	1.576	2.796

condition is beneficial to the dispersion of $KBiFe_2O_5$ nanoparticles, which leads to an enhanced photocatalytic performance.

3　Conclusions

In conclusion, multiferroic $KBiFe_2O_5$ has been successfully prepared by a facile hydrothermal method. The phase purity and morphology were investigated by XRD and FE-SEM. The visible-light absorption was confirmed by UV-Vis spectroscopy. The visible-light-driven photocatalytic performances for degrading RhB and MO can be extremely promoted by decreasing pH value. This finding may provide a new route to improve the photodegradation efficiency of ferroelectric photocatalyst by adjusting the pH value of dyes solution.

References:

[1] CHOI H, SHIN D, YEO B C, *et al*. Simultaneously controllable doping sites and the activity of a W-N codoped TiO_2 photocatalyst. *ACS Catal.*, 2016, **6(5):** 2745–2753.

[2] CHOI H, SOFRANKO A C, DIONYSIOU D D. Nanocrystalline TiO_2 photocatalytic membranes with a hierarchical mesoporous multilayer structure: synthesis, characterization, and multifunction. *Adv. Funct. Mater.*, 2006, **16:** 1067–1074.

[3] LIN JING-CHENG, TANG XIAO, CHU WAN-YI. Synthesis and photocatalysis property of ultra-small TiO_2 nanoclusters in aqueous media. *J. Inorg. Mater.*, 2017, **32(8):** 863–869.

[4] NG K H, CHENG C K. Photo-polishing of POME into CH_4-lean biogas over the UV-responsive ZnO photocatalyst. *Chem. Eng. J.*, 2016, **300:** 127–138.

[5] AKHAVAN O. Graphene nanomesh by ZnO nanorod photocatalysts. *ACS nano*, 2010, **4(7):** 4174–4180.

[6] HSU MU-HSIANG, CHANG CHI-JUNG, WENG HAU-TING. Efficient H_2 production using Ag_2S-coupled ZnO@ZnS core–shell nanorods decorated metal wire mesh as an immobilized hierarchical photocatalyst. *ACS Sustain. Chem. Eng.*, 2016, **4:** 1381–1391.

[7] XUE CHAO, AN HUA, YAN XIAO-QING, *et al*. Spatial charge separation and transfer in ultrathin $CdIn_2S_4$/rGO nanosheet arrays decorated by ZnS quantum dots for efficient visible-light-driven hydrogen evolution. *Nano Energy*, 2017, **39:** 513–523.

[8] CHEN SHAN-SHAN, TAKATA T, DOMEN K. Particulate photocatalysts for overall water splitting. *Nature Rev. Matal.*, 2017, **2(10):** 17050–1–17.

[9] FAN YING-YING, MA WEI-GUANG, HAN DONG-XUE, *et al*. Convenient recycling of 3D AgX/ graphene aerogels (X = Br, Cl) for efficient photocatalytic degradation of water pollutants. *Adv. Mater.*, 2015, **27:** 3767–3773.

[10] ZHANG NING, CHEN DA, NIU FENG, *et al*. Enhanced visible light photocatalytic activity of Gd doped $BiFeO_3$ nanoparticles and mechanism insight. *Sci. Rep.*, 2016, **6:** 26467-1-11.

[11] LI SHUN, LIN YUAN-HUA, ZHANG BO-PING, *et al*. Controlled fabrication of $BiFeO_3$ uniform microcrystals and their magnetic and photocatalytic behaviors. *J. Phys. Chem. C*, 2010, **114:** 2903–2908.

[12] ZHANG GANG-HUA, LIU FENG-LIANG, GU TING-TING, *et al*. Enhanced ferroelectric and visible-light photoelectric properties in multiferroic $KBiFe_2O_5$ *via* pressure-induced phase transition. *Adv. Electron. Mater.*, 2017, **3(3):** 1600498–1–8.

[13] RAMIREZ F, JR E M, SOUZA J A, *et al*, Comprehensive theoretical and experimental study of electrical transport mechanism on $BiFeO_3$ multiferroic nanoparticles. *J. Alloy and Compd.*, 2017, **720:** 47–53.

[14] ZHANG PENG, TENG XIAO-XU, FENG XIANG-HUA, *et al*. Preparation of Bi_2WO_6 photocatalyst by high-energy ball milled Bi_2O_3-WO_3 mixture. *Ceram. Int.*, 2016, **42:** 16749–16757.

[15] ZENG TAO, LOU QI-WEI, BAI YANG, *et al*. Recent progress on the photocatalysis of ferroelectric matrrial. *J. Inorg. Mater.*, 2014, **23(28):** 220–226.

[16] SU R, SHEN Y, LI L, *et al*. Silver-modified nanosized ferroelectrics as a novel photocatalyst. *Small*, 2015, **11(2):** 202–207.

[17] MOHAN S, SUBRAMANIAN B, BHAUMIK I, *et al*. Nanostructured $Bi_{1-x}Gd_xFeO_{3-\alpha}$ multiferroic photocatalyst on its sunlight driven photocatalytic activity. *RSC Adv.*, 2014, **4:** 16871–16878.

[18] GUO JIA, ZHU YI, ZHANG YUAN-MING, *et al*. Hydrothermal synthesis and visible-light photocatalytic properties of $BiVO_4$ with different structures and morphologies. *J. Inorg. Mater.*, 2012, **27(1):** 26–32.

[19] WÜRFEL P, WÜRFEL U. Physics of Solar Cells. Weinheim : Wiley, 2009.

[20] ZHANG GANG-HUA, WU HUI, LI GUO-BAO. New high Tc multiferroics $KBiFe_2O_5$ with narrow band gap and promising photovoltaic effect. *Sci. Rep.*, 2013, **3:** 1265–1–8.

[21] GRINBERG I, WEST D V, TORRES M, *et al*. Perovskite oxides for visible-light-absorbing ferroelectric and photovoltaic materials. *Nature*, 2013, **503(7477):** 509–512.

[22] RANJBARI A, MOKHTARANI N. Post treatment of composting leachate using ZnO nanoparticles immobilized on moving media. *Appl. Catal. B: Environ.*, 2017, **220:** 211–221.

[23] WANG XIONG, LIN YING, DING XI-FENG, *et al*. Enhanced visible-light-response photocatalytic activity of bismuth ferrite nanoparticles. *J. Alloy and Compd.*, 2011, **509:** 6585–6588.

[24] ZHOU YING, ZHANG XIAO-JING, ZHAO ZI-YAN, *et al*. Effects of pH on the visible-light induced photocatalytic and photoelectrochemical performances of hierarchical Bi_2WO_6 microspheres. *Superlattice Microst.*, 2014, **72:** 238–244.

[25] YAO WEI-FENG, XU XIAO-HONG, WANG HONG, *et al*. Photocatalytic property of perovskite bismuth titanate. *Appl. Catal. B: Environ.*, 2004, **52:** 109–116.

[26] SUN YUE, LIU JIA-WEN, LI ZHONG-HUA, *et al*. Design of highly ordered Ag-$SrTiO_3$ nanotube arrays for photocatalytic degradation of methyl orange. *J. Solid State Chem.*, 2011, **184:** 1924–1930.

[27] GUO REN-QING, FANG LIANG, DONG WEN, *et al*. Enhanced photocatalytic activity and ferromagnetism in Gd doped $BiFeO_3$ nanoparticles. *J. Phys. Chem. C*, 2010, **114:** 21390–21396.

[28] ZENG TAO, BAI YANG, LI HAO, *et al*. Fabrication of barium titanate nanophotocatalysts with gridding structures and photocatalytic activities. *J. Inorg. Mater.*, 2015, **30(12):** 1334–1338.

不同 pH 下 $KBiFe_2O_5$ 可见光催化性能研究

李 健[1], 张刚华[2], 范立坤[2], 黄国全[1], 高志鹏[3], 曾 涛[1,2]

(1. 上海电力学院 环境与化学工程学院, 上海 200090; 2. 上海材料研究所 上海市工程材料应用与评价重点实验室, 上海 200437; 3. 中国工程物理研究院 流体物理研究所, 冲击波和爆轰物理国家重点实验室, 绵阳 621900)

摘 要: 采用温和的水热法制备了多铁 $KBiFe_2O_5$ 粉体。利用 X 射线衍射(XRD)和场发射扫描电子显微镜(FE-SEM)等手段对样品的纯度及形貌进行了表征。利用紫外-可见漫反射(UV-Vis DRS)测试了样品的光吸收性能。通过降解罗丹明 B(RhB)和甲基橙(MO)研究了染料溶液 pH 值对 $KBiFe_2O_5$ 可见光催化性能的影响。结果显示, $KBiFe_2O_5$ 的可见光催化性能随着溶液 pH 值的下降而显著提升, 这是由于溶液中的催化剂在酸性条件下具有更好的分散性, 并且染料分子更容易吸附到催化剂表面, 从而提高催化效率。

关 键 词: $KBiFe_2O_5$; 光催化剂; 可见光照射; pH

中图分类号: X703 **文献标识码:** A